Extended Abstracts of the 16th (1984 International) Conference on Solid State Devices and Materials, Kobe, 1984, pp. 121-124

C-1-2

Invited

Focused Ion Implantation for Optoelectronic Integrated Circuits

Hisao Hashimoto and Eizo Miyauchi

Optoelectronics Joint Research Laboratory

1333 Kamikodanaka, Nakahara-ku Kawasaki 211, Japan

Maskless ion implantation using focused ion beams and its application to MBE for an OEIC fabrication process are described. Fine patterned p(Be)- and/or n(Si)-type ion implanted GaAs layers with less lattice damage were formed arbitrarily by changing electric field of an ExB mass separator using an Au-Si-Be LM ion source. The novel MBE system combined with this implanter in UHV was constructed to grow three dimentional doping epitaxial layers, and was confirmed to have good performance in the preliminary GaAs growth.

1. Introduction

A submicrometer focused ion beam(FIB) has recently received a great deal of attention as a technique for a microfabrication process of semiconductor devices.1-5) The most promised use of it is for maskless ion implantation. This technology has various advantages over the conventional ion implantation. Selective ion doping with very fine patterns can be formed without a photolithography process through computer software. The application of maskless ion implantation doping to a crystal growth process will also open up possibilities for a new crystal growth technique. It is suitable to fabricate the intricated crystal structures for optoelectronic integrated circuits (OEIC's).

For the fabrication of OEIC's, different structural elements must be monolithically integrated on a substrate.6) They involve great difficulties in device fabrication, in particular, of the planar structural devices. The crystal growth process is a necessary step for the realization of planar type OEIC's, which need the multilayer structure of III-V compound crystal selectively doped with p- and n-type impurities. The best way to overcome the present technical level is to use a new crystal growth method by molecular beam epitaxy(MBE) combined with maskless ion implantation.

We have studied maskless ion implantation using FIB to apply this technology to MBE. Recently, a novel MBE system coupled with a maskless ion implanter in an ultrahigh vacuum(UHV) was constructed.7) In this report, some experimental results of FIB implantation in GaAs and feasibility about the application of FIB doping to MBE for OEIC's are shown and discussed.

2. Focused ion implantation

2.1 Implatation system

Figure 1 shows a schematic structure of the 100 keV maskless ion implanter.4) The focusing column is consisted of a field emission liquid metal(LM) ion source, a three-electrodes-type condenser lens and an Einzel-type objective lens with an ExB mass separator and a postlens deflector. This implanter can focus ion beams down to smaller than 0.1 um in diameter. The focused ion beam is scanned in x and y directions with a deflector.

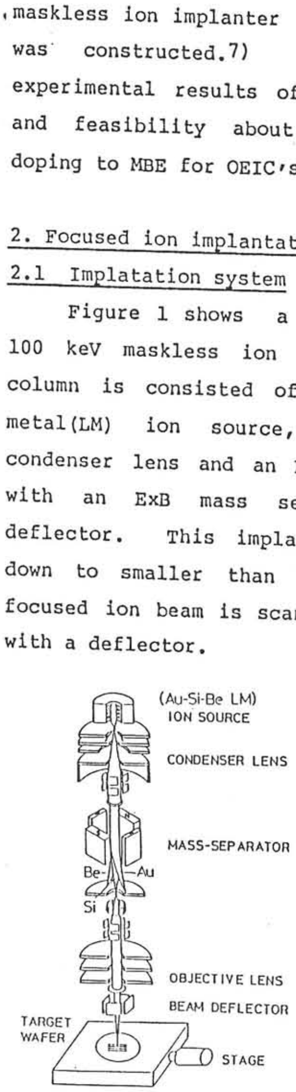

Fig.1 Schematic structure of 100kV maskless-ion implanter.

Using the Au-Si-Be (65:27:8 atom. %) LM ion sourece,[8] which emits both p-(Be) and n-(Si) type ion beams from one tip, Be and/or Si ions can be implanted arbitrarily by merely switching the electric field of an ExB mass separator. Ion species are interchangeable without the cumbersome source changing procedure which usually includes breaking the vacuum and readjustment of ion optics. These implantation procedures are carried out smoothly under computer control. Lateral doping profiles also can be formed at will by varying dwell time as the beam is scanned across a target.

2.2 Doping profile

FIB implantation is capable of forming fine doping patterns of impurities. However, it must be noted that implanted ions are scattered and spreaded in crystal through collisions with the nuclei of crystal. Fig. 2 shows calculated contours of equi-ion-concentration in the Be and Si line-implanted GaAs at 160 keV with the dose of 1×10^{13} cm^{-2} using FIB with 0.1 um full width at 1/e maximum of the assumed-Gaussian intensity distribution. When the impurity concentration level of the substrate is 1×10^{15} cm^{-3}, the estimated line widths of the Be and Si implanted regions are about 1 um and 0.5 um respectively.

The photograph in Fig.3 is a SEM image of the doubly charged Si implanted n-type, (100) GaAs (1×10^{15} cm^{-3}) with 7° off the axis under the same condition as a calculation in Fig.2. In this sample, the n-type GaAs layer(1×10^{15} cm^{-3}) of 1.5 um was grown on the implanted layer by MBE to reduce the influence of thermal conversion of the surface region during annealing of the sample with SiO_2 encapsulant at 800 °C for 20 min. The line doped with Si is around 0.4 um in width as shown in Fig. 3. Close agreement between observed and calculated value was obtained. A lateral spread depends on ion energy and dose, too. The line width becomes narrower in proportion as both ion energy and dose decrease.

2.3 Implant damage

In FIB implantation, very high-density ion beams which are 10^3 to 10^6 times greater than unfocused ion beams(UIB's) by a conventional implanter are used. Such high-density ion beams affect the generation of lattice damage in the implanted crystal.[9-12] In applying FIB implantation to a crystal growth and a device fabrication process, it is important to

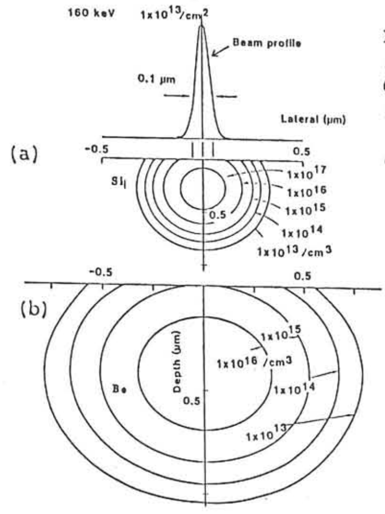

Fig.2. Contours of equi-ion-concentration in GaAs for as line-implanted (a)Si and (b)Be at 160keV to a dose of $1\times10^{13}cm^{-2}$.

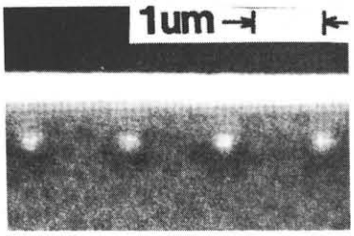

Fig.3. Cross-section SEM image for the Si line-implanted GaAs under the same condition with Fig.2

investigate the damage generation.

In order to characterize the implant damage, the 160 keV Be FIB's of o.2 um diameter with beam current of 90 pA were raster-scanned over the 400 um square area of n type (100) MBE GaAs(2.7×10^{15} cm^{-3}) at a speed of 10 cm s^{-1} with the dose of 3×10^{14} cm^{-2}. The damage depth profiles in the implanted layer were obtained by Raman scattering measurement in conjunction with step-etching of the sample.[10] The frequency shift of LO phonon line due to lattice strain in GaAs represents amount of damage.[9]

In Fig. 4, the depth distribution profile is depicted as compared with that of UIB implantation. The ordinate represents the difference of the frequency shift between the implanted(denoted by ω_{impl}) and the unimplanted GaAs(denoted by ω_{unimpl}, 291.9 cm^{-1}). This value corresponds to the degree of implant damage. The significant reduction of FIB implant damage for FIB compared with UIB at the near-surface region was observed. This result strongly suggests that damage annealing occurs during FIB implantation, in particular, at the near-surface region. However, it was reported that the temperature of the target being FIB implanted rose to unacceptable levels. The same damage reduction in the Si FIB implanted GaAs layer was observed.[9]

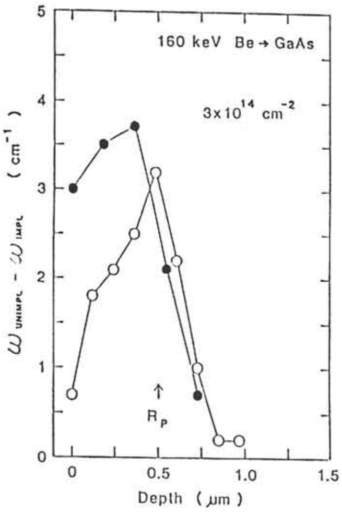

Fig.4. Depth distribution profiles of damage in Be implanted GaAs. The ordinate represents the difference of the frequency shift between the implanted and the unimplanted GaAs.

o: FIB

•: UIB

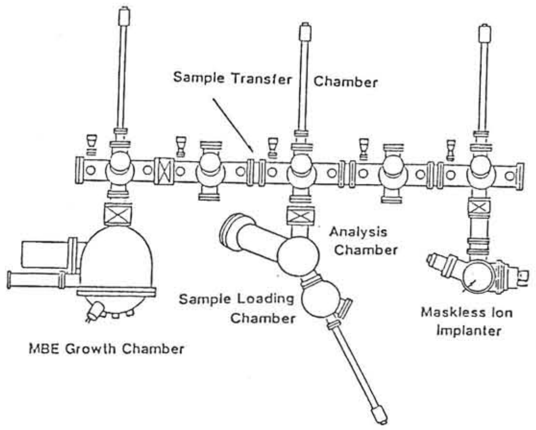

Fig.5 Schematic structure of the MBE system with the 100kV maskless ion implanter.

These damage reductions somewhat differed from the data of the B and Ga implanted Si layers at relatively low energy,[11,12] which resulted in an enhanced damage generation.

Energy transfer of projectile ions via the electronic excitation of target atoms is more predominant than that via collisions with target nuclei at the surface region under the present implantation condition. Accordingly, it is considered that a high rate of localized electronic energy transfer to disordered lattice atoms possibly contributes to the damage reduction,[10] through dense formation of electron-hole pairs by FIB implantation, followed by recombination at damages.[13]

The electrical characteristics of the FIB implanted layers after high temperature annealing are superior to those doped with UIB because of the damage reduction during implantation.

3. Application to crystal growth

3.1 Growth system

Maskless ion implantation technique was applied to MBE for patterning to three dimensions by FIB implantation during crystal growth. Crystal quality of GaAs and its related compound at the interface, where the MBE growth is interrupted, is remarkably degraded with interface states once the growing crystal surface is exposed to the atmosphere.[14] In order to prevent such a trouble, the MBE growth chamber was connected with the 100 kV maskless ion implanter through the sample transfer chamber of UHV. A schematic structure of the combined growth system is shown in Fig. 5. The arbitrarily pattern-doped three dimensional epitaxial layers can be grown in a vacuum below $5x10^{-10}$ Torr by transferring the growing crystal between the MBE growth chamber and the implanter using the magnetic coupled transfer rods and the small truck.

3.2 Be implanted GaAs MBE

Be doped GaAs with FIB implantation was grown and characterized by measuring photoluminescens (PL) intensity depth profiles in the grown crystal. The sample structure is shown in Fig.6. At first, p-type GaAs($1x10^{16}$ cm^{-3}) doped with Be using an effusion cell was grown on semi-insulating (100) GaAs to a thickness of 2.4 um at 600 °C, and then, the 160 keV Be FIB's were raster-scanned over the 5 mm square area with the dose of $1x10^{13}$ cm^{-2}. Subsequently, p-type GaAs of 1.2 um in thickness was grown again on the implanted layer without high temperature annealing. After growth, the sample was taken out from the growth system, and then annealed at 850 °C for 20 min with SiO_2 encapsulation.

Fig. 7(a) shows the PL depth profiles measured at A(unimplanted) and B(Be-implanted) regions in Fig. 6. No decrease in PL intensity at the interface, where the MBE growth was interrupted during ion implantation, was detected, regardless of Be implantation. This result also confirms that damages induced by Be implantation do not affect interface crystallinity of MBE grown GaAs without high temperature annealing after

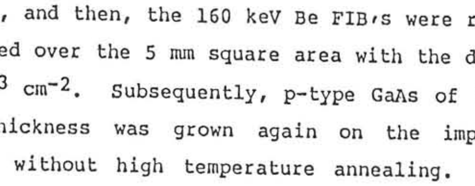

Fig.6 Schematic cross section of the selectively Be implanted GaAs. PL was measured in the indicated direction.

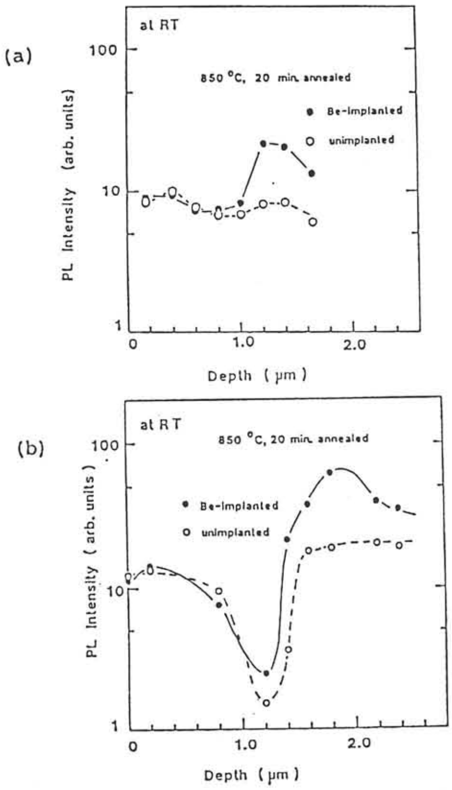

Fig.7 Depth profiles of PL in (a) the Be implantation doping MBE GaAs using the new system shown in Fig.5 and (b) the samples purposely exposed to the atmosphere before Be implantation.

implantation. The lattice disorders produced by implantation doping were almost annealed out at the initial stage of the subsequent MBE growth procedure at around 600 °C.[7] This means that the selectively ion implanted MBE multilayers where lasers, photodiodes, FET's, and other elements are integrated monolithically, can be annealed to activate doped impurities after all growth is completed. It is favourable to fabricate OEIC's.

The comparison sample, which was purposely exposed to the outer atmosphere before Be implantation, showed a remarkable decrease in PL intensity near the regrown interface as shown in Fig. 7(b). This phenomenon is similar to carrier depletion at the interface of MBE GaAs, reported previously.[14]

On the other hand, PL intensity in the Be implanted layer was about one-fifth of intensity for MBE grown GaAs doped with the same Be concentration using an effusion cell, though annealing condition was not optimized. This PL intensity will be increased further by optimizing annealing condition.

4. Conclusion

Maskless ion implantation using focused ion beams offers a new tool for impurity doping. Fine patterned implantation doping in GaAs with p- and/or n-type impurity was performed at will by changing the electric field of an ExB mass separator using the Au-Si-Be LM ion source. There was no trouble of high current-density implantation. Damages in the implanted GaAs layers with Be and Si decreased in comparison with those induced by a conventional implanter. The novel MBE system combined with this maskless ion implanter was constructed, to fabricate the intricated structural crystal for OEIC's. Preliminary results of the GaAs growth showed that this system was capable of growing a good quality selectively doped crystal

Acknowledgements

We thank Drs. T. Iizuka M. Hirano and I. Hayashi of Optoelectronics Joint Research Laboratory for encouraging this work.

The present research effort is part of a major reseach and developement project on optical measurement and control systems, conducted under a program set up by the Ministry of International Trade and Industry's Agency of Industrial Science and Technology.

References

1) R.L.Seliger, J.W.Ward, V.Wang and R.K.Kubena: Appl. Phys. Lett. 34(1979) 310.
2) R.L.Kubena, J.Y.Lee, R.A.Jullens, R.G.Braut, P.L.Middleton and E.H.Stevems: IEDM-1983 Tech. Digest(1983) p.566.
3) W.L.Brown and A.Wagner: Proc. Int. Ion Engeneering Congress, Kyoto(1983) p.1738.
4) E.Miyauchi, H.Arimoto, H.Hashimoto and T.Utsumi: J.Vac.Sci.Technol. B1(4)(1983) 1113.
5) T.Shiokawa, P.H.Kim, K.Toyoda, S.Namba, T.Matsui and K.Gamo: J.Vac.Sci.Technol. B1(4)(1983)1117.
6) N.Bar-chaim, S.Margalit and A.Yariv: IEEE Trans. Electron Devices, ED-29(1982)1372.
7) A.Takamori, E.Miyauchi, H.Arimoto, Y.Bamba and H.Hashimoto: to be published.
8) E.Miyauchi, H.Hashimoto and T.Utsumi: Jpn.Appl.Phys. 22(1983) L225.
9) Y.Bamba, E.Miyauchi, H.Arimoto, K.Kuramoto, A.Takamori and H.Hashimoto: Jpn.J.Appl.Phys. 22(1983)L650
10) Y.Bamba, E.Miyauchi, H.Arimoto, A.Takamori and H.Hashimoto: to be published in Jpn. J.Appl.Phys.
11) R.R.Hart, C.L.Anderson, H.L.Dunlap, R.L.Seliger and V.Wang: Appl.Phys.Lett. 35 (1979)865.
12) M.Tamura, S.Shukuri, S.Tachi, T.Ishitani and H.Tamura: Jpn.J.Appl.Phys. 22(1983) L698.
13) D.V.Lang and L.C.Kimerling: Phys. Rev.Lett. 33(1974)489.
14) N.J.Kawai, C.E.C.Wood and L.F.Eastman: J. Appl.Phys. 53(1982) 6208.